PCCP

Accepted Manuscript

ROYAL SOCIETY OF CHEMISTRY

www.rsc.org/pccp

Nanoparticles of CoAPO-5: synthesis and comparison with microcrystalline samples

Serena Esposito[1*], Barbara Bonelli[2], Marco Armandi[2], Edoardo Garrone[2] and Guido Saracco[2]

[1]*Department of Civil and Mechanical Engineering, Università degli Studi di Cassino e del Lazio Meridionale, Via G. Di Biasio 43, 03043 Cassino (FR), Italy.*

[2]*Department of Applied Science and Technology and INSTM Unit of Torino-Politecnico, C.so Duca degli Abruzzi 24, Politecnico di Torino, I-10129, Torino, Italy.*

* Dr. **Serena Esposito**, *Department of Civil and Mechanical Engineering, Università degli Studi di Cassino e del Lazio Meridionale, Via G. Di Biasio 43, 03043 Cassino (FR), Italy.*

E-Mail: s.esposi@unicas.it

Abstract

The hydrothermal synthesis of a nanosized cobalt doped aluminum phosphate CoAPO-5 (CoAPO-5-N) in a water/surfactant/organic solvent mixture (emulsion method) is reported, along with its physico-chemical characterization and comparison with a sample obtained by conventional synthesis (CoAPO-5-C).

Both XRD (X-Ray Diffraction) peak widths and FESEM (Field Emission Scanning Electron Microscopy) pictures of CoAPO-5-N are in agreement with a nanoscale structure, although aggregation of nanoparticles occurred. EDX analysis shows a more homogeneous distribution of cobalt in CoAPO-5-N, not attainable by conventional synthesis. The specific surface area, as measured by nitrogen adsorption at 77 K, shows a limited increase in CoAPO-5-N (242 m^2/g) with respect to CoAPO-5-C (216 m^2/g), whereas the external surface area is almost tripled. Such definite increase in the outer surface of CoAPO-5-N is also evidenced by the fourfold increase in the rate of a reaction only involving the exterior surface of particles, the light-driven oxidation of water by persulfate anions, as activated by the bulky $Ru(bipy)_3^{2+}$ complex, is unable to enter CoAPO-5 micropores.

Two new features were also noted, adding to the knowledge of CoAPO-5 systems: i) tetrahedral Co^{3+} species may coordinate ammonia molecules, assuming a octahedral configuration, as determined by UV-Vis spectroscopy; ii) Co^{2+} species in trigonal coordination occur, able to coordinate either CO molecules at a low

temperature or ammonia (or water) at room temperature, as evidenced by IR and UV-Vis spectroscopy, respectively.

1. Introduction

Porous aluminum phosphate solids in which a transition metal (Me) partially substitute for Al (MeAPO systems) have enjoyed much popularity in the past as potential redox catalysts,[1-6] when changes in oxidation number (ON) at the Me centre are possible. Interestingly, changes in the ON of Me centres involve simultaneous formation/depletion of Brønsted acidic centres (Scheme 1).

Although great expectations in their catalytic potentialities have not been entirely fulfilled, such systems are still of interest. For instance, we have recently reported that Co^{3+} ions in activated CoAPO-5 react with liquid water at room temperature,[7] yielding O_2 according to the reaction:

$$4\ Co^{3+} + 2\ H_2O \rightarrow 4\ Co^{2+} + 4\ H^+ + O_{2(g)} \qquad (1)$$

After water contact, Co ions capable of undergoing changes in ON may be brought to react under visible light irradiation, either electrochemically [8] or by the use of a sacrificial reactant.[9] In the former case, CoAPO-5, when incorporated into Nafion films on conductive layers, behaves simultaneously as a water oxidation (WO) catalyst and a visible light photosensitizer.[8] In the latter case, activity of CoAPO-5 in WO has been measured in a flow reactor in the presence of a sensitizer $[Ru(bpy)_3]^{2+}$ and a sacrificial reagent ($S_2O_8^{2-}$).[9]

Such findings make CoAPO-5 interesting from the viewpoint of water splitting (WS), a reaction much studied for its potential applications in the storage of solar energy into chemical bonds.[8-10]

Because in the cases above the porous nature of CoAPO-5 may hamper diffusion, we have been brought to consider the same system with a larger outer surface. To this purpose, attempts have been made in the past to either introduce hierarchical porosity, or synthesize nanosized particles.[11-13] The latter have failed, and at the most crystals nano-sized only in one direction (whiskers) have been obtained.[13]

An alternative, so far unexplored way could be the emulsion method successfully applied to the preparation of nanosized MFI- and MOR-type zeolites.[14-16]

It has been noted that literature has made clear that the chemistry of MeAPO, and of CoAPO-5 in particular, is far more complex than a plain isomorphic substitution of tetrahedral Al by another metal. Scheme 2 illustrates the various species that are thought to occur: in the as prepared sample, Co^{2+} ions substitute for some Al^{3+} species, the resulting negative net charge being balanced by the positive charge of a protonated template molecule. Removal of the latter, *e.g.* by thermal oxidative treatment, leads to both the oxidized species A, featuring Co^{3+}, and the un-oxidized species B, featuring Co^{2+} and a hydroxyl bridging between such Co^{2+} ion and a P atom (Co^{2+}–(OH)–P). Species B, however, are not thermally stable and tend to dehydrate, which simultaneously yields species C and D: the former is a coordinatively saturated Co^{2+} ion, the latter is the same, but with a coordination vacancy, making the cation tri-coordinated and prone to adsorb molecules (Scheme 3).

The present work reports an attempt to use the emulsion method for the synthesis of nanosized CoAPO-5 particles, along with the rather thorough characterization of the obtained sample (hereafter referred to as CoAPO-5-N) and the measurement of its Oxygen Evolution (OE) ability in the WS reaction with a sacrificial reactant.

2. Experimental

2.1 Synthesis

The synthesis of CoAPO-5-N by emulsion method involved two phase: the organic one was obtained by dissolving a surfactant, polyoxyethylene-10-oleyl ether (Sigma-Aldrich), into cyclohexane (Merck). Three surfactant concentrations were explored, namely 0.25, 0.50 and 0.75 mol/L.

Preparation of the second phase started from an aqueous solution of Co^{2+} acetate tetrahydrate (Sigma-Aldrich), to which aluminium isopropoxide (Sigma-Aldrich) and, then, phosphoric acid (Merck, 85 wt%) were slowly added, the resulting mixture being stirred for 1 h at room temperature (r.t.). After addition of DEA (N,N-diethylethanolamine, Sigma-Aldrich, 99.5%), the purple mixture underwent further stirring for 1 h. The molar composition of the gel was 0.96 Al_2O_3 : 1.0 P_2O_5 : 0.08 CoO : 1 DEA : 60 H_2O, to which corresponds a nominal cobalt content of 1.9 wt% in the final product, $Co_{0.02}Al_{0.48}P_{0.5})O_2$

10 cc gel mixture was slowly added to 70 cc organic solution: the resulting mixture was stirred for 2 h, then placed in a Teflon lined stainless steel autoclave, and heated to 448 K for 24 h. The crystalline products were filtered, washed with 2-propanol (Sigma-Aldrich, anhydrous 99.5%) and dried at 343 K for 48 h. Both the surfactant and the organic template were finally removed by calcination under flowing oxygen at 823 K.

For comparison, CoAPO-5 materials were prepared by hydrothermal synthesis at 473 K for 24 h (hereafter referred to as CoAPO-5-C, C for conventional), without addition to any surfactant/organic solvent mixture. Three samples of CoAPO-5-C $(Co_xAl_{0.5-x}P_{0.5})O_2$ with different Co content (3.0, 1.9, and 0.96 wt.%) were prepared, one with the same gel composition of CoAPO-5-N (Table 1).

2.2 Characterization.

Powder X-Ray Diffraction (XRD) patterns were obtained on a X'Pert Phillips diffractometer operating with Cu Kα radiation (1.541874 Å) in the 2.5 – 18° 2θ range (step width = 0.02°, time per step: 2.00 s) and were indexed according to the JCPDS database. The average size of crystallites was determined from XRD patterns by means of the Debye-Scherrer formula: $D = 0.9\lambda/b \cos\theta$, where λ is the wavelength of the Cu Kα radiation, b is the peak full width at half maximum (in radians), 0.9 is the shape factor for spherical particles and θ is the diffraction angle.

Field Emission Scanning Electron Microscopy (FESEM) pictures were taken on a ZEISS Supra 40 Field Emission Scanning Electron Microscope. The same

instrument is equipped with an EDX (Electron Dispersive X-ray) probe that was used to determine the samples chemical composition on 10-50 nm diameter spots.

N_2 isotherms at 77 K were measured on samples previously outgassed at 523 K, to remove atmospheric water and other atmospheric contaminants (Quantachrome Autosorb 1). Specific surface area (SSA) values were calculated according to both the BET (Brunauer-Emmett-Teller) and the Langmuir method; total pore volumes were determined from adsorbed amounts at $P/P^0 = 0.98$; both micropore volume and external surface area were calculated according to the *t*-plot method.

Diffuse Reflectance (DR) UV-Vis spectra of powders were measured on a Cary 5000 UV-Vis-NIR spectrophotometer (Varian instruments), equipped with an integration sphere, in a UV-Vis cell allowing the dosing of gaseous ammonia at r.t.. The obtained DR-UV-Vis spectra are reported as Kubelka-Munk function, F(R), versus wavelength (nm).

For IR measurements, samples were shaped into thin, self-supporting wafer and outgassed at 523 K in a vacuum frame (residual pressure below 10^{-3} mbar). IR spectra were taken both of the samples as such and after dosage of CO at the nominal NBP of nitrogen, in a home-made IR cell, allowing to carry out thermal treatments and successive dosing of gases. Fourier Transform (FT) IR spectra were recorded at 2 cm^{-1} resolution on a Bruker Equinox 55 spectrophotometer equipped with a MCT (mercury cadmium telluride) cryodetector.

2.3 Oxygen evolution measurements

To measure the ability of the catalyst to promote light-driven water oxidation

$$n\ h\nu + H_2O_{(l)} \rightarrow 4\ H^+_{(aq)} + 4\ e^- + O_{2(g)} \qquad (2)$$

an oxidizing sacrificial reagent was used, the persulfate anion $S_2O_8^{--}$,the resulting reaction being:

$$n\ h\nu + 2\ S_2O_8^{--}{}_{(aq)} + 2\ H_2O_{(l)} \rightarrow O_{2(g)} + 4\ SO_4^{--}{}_{(aq)} + 4\ H^+_{(aq)} \qquad (3)$$

Hydronium ions are given rise, so that a buffer system is present. Light energy is harvested by means of the dye, Tris(2,2'-bipyridyl)Ru(II) chloride, hereafter referred as $[Ru(bpy)_3]^{2+}$.[9,10]

OE was measured by means of a bubbling reactor, where O_2 is simultaneously monitored both in the liquid and in the gaseous phase.[10] A typical reaction mixture contains: 100 mg catalyst; 130 ml of buffer hexafluorosilicate 50 mM (Na_2SiF_6 22 mM + $NaHCO_3$ 28 mM; starting pH = 5.5); Na_2SO_4 20 mM; $Na_2S_2O_8$ 5 mM, and $[Ru(bpy)_3]^{2+}$ 0.5 mM . During the experiment, Argon was fluxed at 12 Nml/min^{-1} and the solution was stirred at 1100 rpm; pressure and temperature were 1.08 bar and 293 K, respectively. Prior to each measurement, the system was purged by flowing Ar in dark condition. Then, the reactor was illuminated through the quartz window with simulated solar light (100 mW/cm^2) by using a plasma lamp by Solaronix (model LIFI STA-40).

3. Results and Discussion

3.1 Morphological and textural properties

The surfactant concentration resulted to be a key parameter in the synthesis under study as any attempt to crystallize CoAPO-5 samples with a surfactant concentration higher than 0.25 mol/L was unsuccessful.

Figure 1 reports the XRD pattern of CoAPO-5-N, as obtained by using a surfactant concentration equal to 0.25 mol/L, which shows good crystallinity of the AFI phase (JCPDS file 41-0044): an exagonal arrangement of Al and P in tetrahedral coordination, (space group P6cc, a = b = 1.37 nm) Peak widths yield, through the Debye-Scherrer formula, an average size of crystallites of 60 nm, *i.e.* much smaller than the size of the CoAPO-5-C crystallites with the same cobalt content. A FESEM image of this latter, reported in Figure 2a, shows well developed micron-sized hexagonal prisms. A FESEM image of CoAPO-5-N (Figure 2b) shows instead large aggregates of nanoparticles (NPs) with average dimensions of about 70 nm. This seems to suggest that the synthesis of CoAPO-5-N was successful.

Adsorption/desorption isotherm of N_2 for CoAPO-5-N and CoAPO-5-C are of type I according to the IUPAC classification, both corresponding to that expected for a microporous system with a small contribution from mesopores (data not reported). Table 1 reports textural data for CoAPO-5-N and for the set of CoAPO-5-C samples with different Co content, a parameter which definitely affects SSA: as expected, Langmuir SSA values are slightly larger than BET values, but the trend is the same

along the series, *i.e.* in the CoAPO-5-C series SSA increases with the Co content. The comparison, however, between CoAPO-5-N and CoAPO-5 with the same Co content shows that SSA of CoAPO-5-N is slightly larger, whereas the external surface is almost tripled in the sample prepared by emulsion method.

The ensemble of the above results seems to indicate that CoAPO-5-N NPs have indeed been prepared as a result of the emulsion synthesis, but that successive thermal history has brought about the sintering of the NPs finally occurring as aggregates, rather than dispersed NPs .

3.2 Comparison of chemical properties

EDX measurements of the Co concentration at different points of the particles indicate that the distribution of cobalt in CoAPO-5-N is definitely more homogenous than in CoAPO-5-C, so yielding support to the idea that the synthesis mechanism involves pristine identical NPs eventually sintered. Table 2 reports the Co wt% determined on different spots.

As prepared powders of both CoAPO-5-N and CoAPO-5-C have the typical blue color of tetrahedral Co^{2+} complexes, turning gray-greenish after calcination in O_2, because some Co^{2+} ions were oxidized to Co^{3+}.[3, 17-18] Fig. 3 a reports the DR UV–Vis spectra of CoAPO-5-N after r.t. drying (black solid line), calcination (dashed line) and outgassing at 423 K (grey solid line). The dried sample shows the triplet due to the $^4A_2$ (F)-$^4T_1$ (P) transition of Co^{2+} ions in tetrahedral environment, occurring at 540, 580 and 629 nm when template is present.[7,19] The relatively weak

peak at 250 nm is due to APO-5 structure, being present in the pure phase (resulted non reported).

The calcined sample (dashed line) features a broad UV band in the range 300-400 nm, due to oxygen ligand-to-metal charge-transfer bands of Co^{3+} in tetrahedral coordination,[18] the corresponding d-d transitions being instead masked by the more intense absorptions of Co^{2+} ions.[3, 20-21] Oxidation of Co^{2+} to Co^{3+} is limited to a 15-20 % of the total cobalt content, as suggested by the residual intensity of the triplet and in agreement with the literature in the field.[7, 22] Consider that, before outgassing, type-D sites most probably still carry water molecules, so contributing to the triplet intensity. The UV-Vis spectrum of the calcined sample outgassed at 423 K monitors the loss of water from tetrahedral sites, leading to a trigonal distortion of the ideal tetrahedral symmetry. The formation of trigonal pyramidal cobalt centers leads causes the modification of the triplet profile.[23-24] Corresponding UV-Vis spectra for the sample CoAPO-5-C in Fig. 3b show no relevant differences with respect to CoAPO-5-N.

IR spectra concerning the hydroxyl stretching region of CoAPO-5-N and CoAPO-5-C do not bring into evidence any relevant differences between the two materials. More meaningful are the IR spectra of the two samples outgassed at 423 and 523 K in the 975-800 cm^{-1} region, where framework vibrations occurs, reported in Fig. 4 for CoAPO-5-N (curves 1 and 2) and CoAPO-5-C (curves 3 and 4), respectively. With both samples, outgassing at 523 K (solid curves) brings about the intensification of a weak band at about 915 cm^{-1}, already present after outgassing at

423 K (dotted curves). A similar band, found on CoAPO-18,[2] was assigned to the symmetric stretching vibration of Co^{2+} - O bonds of trigonal species D (Scheme 3): the same band should have a counterpart at higher wavenumbers assigned to the related asymmetric stretching vibration (950-940 cm^{-1}), which cannot be appreciated in the present case due to the strong IR absorption of the samples in that region. Both such bands should disappear when trigonal species D coordinate another ligand, for instance a CO molecule.

Figures 5 and 6 report IR spectra, in the CO stretching region, as obtained after dosing carbon monoxide on CoAPO-5-N and CoAPO-5-C outgassed at 523 K, respectively. In both figures, difference spectra are reported, as obtained after subtraction of spectra of the bare samples in Fig. 4; insets refer to the framework vibrations range.

CO adsorbed on CoAPO-5-N outgassed at 523 K brings about the formation of several bands in the 2225-2050 cm^{-1} range (Fig. 5): a weak band at 2208 cm^{-1} is assigned to CO molecules interacting with some Co^{3+} species,[25, 26] the most intense band at 2186 cm^{-1} to CO adsorbed on extra-framework Co^{2+} ions.[7]

The band at 2186 cm^{-1} has two (minor) components at 2194 and 2182 cm^{-1} that are ascribable to carbon monoxide adsorbed on Co^{2+} ions in slightly different environments. The former is tentatively assigned to CO interacting with trigonal species D, that because of the coordination vacancy should polarize efficiently CO molecules, so that the corresponding band is expected at higher wavenumbers (2194

cm^{-1}). Inset to Fig. 5 shows indeed a negative band forming when the partial pressure of CO increases, likely due to the coordination of CO molecules by trigonal species D: the Co^{2+} - O band, originally observed at 915 cm^{-1}, disappears upon CO dosage, because trigonal species are turned into tetrahedral ones.

The component at 2182 cm^{-1} is likely due to CO molecules on Co^{2+} clusters. Co ions in framework positions in CoAPO-5 are known to form Co–O–P–O–Co clusters with five or six neighboring Co atoms,[27] where Co ions may alternate between the divalent and trivalent states. At higher CO partial pressures, a band at 2164 cm^{-1} is seen (asterisk), due to CO molecules interacting by H-bonding with slightly acidic hydroxyls of B bridged species: note that the frequency value is indicative of the acidic nature of the Co^{2+}– (OH)–P groups. At lower wavenumbers, two minor bands are observed at 2085 and 2075 cm^{-1}: they are tentatively assigned to $Co(CO)^{\delta+}$ carbonils in a lower oxidation state, as previously observed.[28] Finally, at higher CO partial pressures, a band at 2139 cm^{-1} is readily assigned to the liquid-like phase commonly found when CO is dosed on microporous materials.

Comparison with CoAPO-5-C shows the following differences: (i) no band is seen at 2164 cm^{-1}; (ii) the relative intensity of the band at 2182 cm^{-1} is slightly higher as compared to CoAPO-5-N, indicating that by conventional synthesis the formation of cobalt clusters is slightly favored and (iii) bands ascribed to CO adsorbed on reduced cobalt species (2085 and 2075 cm^{-1}) are more intense, indicating again the

formation of Co clusters, because reduction is likely to imply the removal of oxygen from adjacent Co cations.

Figure 7 reports UV-Vis spectra concerning the interaction of CoAPO-5-N outgassed at 423 K with gaseous ammonia at r.t. Adsorption of ammonia causes two main changes in the spectrum: on the one hand, the component at *ca.* 656 nm, due to D trigonal species, disappears to the increase of the triplet intensity, because the latter species assume a tetrahedral coordination. On the other hand, the broad band centered at 340 nm related to Co^{3+} markedly decreases. Note however that such band is not depleted at any ammonia pressure, as a component at 415 nm is still observed. The observed effects are reversed by mild outgassing at r.t. The almost total disappearance of the broad band is due to the expansion of the coordination sphere of tetrahedral Co^{3+}, caused by addition of ammonia to a octahedral final configuration. The related UV-Vis d-d band, assigned to the transition $^1A_{1g}$ -$^1T_{2g}$, are expected to fall at *ca.* 410 nm, [19, 29-30] and to be weaker than those of tetrahedral Co^{3+}, which explain the persistence of what may be mistaken for a residue of a pristine band.

The results concerning CoAPO-5-C are entirely similar. In conclusion, all evidence is that the bulk chemical features of the two samples do not differ sizably. The following shows that, instead, surface features are different.

The possibility of expanding the coordination sphere by means of a strong ligand like ammonia is in agreement with the possible mechanism of the spontaneous oxidation of water by Co^{3+} in CoAPO-5 systems (reaction 1). If a similar expansion

takes place in the presence of liquid water, the central Co^{3+} ion would be surrounded by two water molecules and four oxygen ligand, a situation rather close to that of the octahedrally coordinated cation $Co(H_2O)_6^{3+}$, which is unstable and oxidizes water.[30]

3.3 Activity in Water Oxidation

Being interested in the effect of an increase of external surface area due to nanostructuration of the CoAPO-5, $[Ru(bpy)_3]^{2+}$ / $S_2O_8^{2-}$ photosystem was used to compare the activity of CoAPO-5-N and CoAPO-5-C in WO reaction, in similar conditions to those previously reported. [9]

Figure 8 compares the time course of OE evolution when catalysed by either CoAPO-5-N (circles) or CoAPO-5-C (triangles) with the same content. Control experiment (crosses) in the absence of any catalyst was also performed, showing negligible amounts of evolved O_2. A description of the complex reactions taking place, also involving degradation of the Ru complex, is given elsewhere.[9,10] The cumulative OE indicate that activity for CoAPO-5-N is *ca.* fourfold than that of CoAPO-5-C. The first reason is clearly that, because of the bulkiness of the Ru complex, OE reaction can only take place at the outer surface of the catalyst, which has a different development in the two cases. Indeed, those cobalt ions exposed to the external surface of CoAPO-5 particles may be accessible to the bulky dye molecule, thus being active in visible light driven WO. However, there is not a perfect quantitative correspondence between the increase of water oxidation activity and the

external surface area. The more homogeneous distribution of Co in the CoAPO-5-N structure evidenced by FTIR spectroscopy and EDX measurement contributes to the higher activity of the nanostructured sample.

4. Conclusions

The attempt to synthesize nanosized CoAPO-5 particles via the emulsion method has proved to be successful. However, the system arrived at is not describable as mono-dispersed CoAPO-5 nanocrystals, because NPs given rise sinter in the final thermal treatments. Indeed, both XRD peak widths and FESEM pictures are in agreement with a nanoscale structure.

The most relevant differences between CoAPO-5-N and CoAPO-5-C concern the outer surface area and the distribution of Co ions: the former shows a substantial increase in CoAPO-5-N with respect to the sample obtained by conventional synthesis; the latter is more homogeneous in the nanostructured sample because the different nucleation and growth mechanism in the two systems. Such features of CoAPO-5-N brings about a fourfold increase in the rate of a reaction only involving the exterior of particles, the light-driven oxidation of water by persulfate anions activated by the bulky $Ru(bpy)_3$ complex, unable to enter CoAPO-5 micropores. The larger development of the outer surface together with a more homogeneous distribution of cobalt may prove to be useful in the use of CoAPO-5 as water oxidation catalyst.

Finally, the physico-chemical characterization of the newly synthesized sample allowed figuring out two new features, adding to the knowledge of CoAPO systems: (i) tetrahedral Co^{3+} species may coordinate ammonia by assuming a octahedral configuration, as revealed by DR-UV-Vis spectroscopy, and (ii) Co^{2+} species coordinating either CO, water and NH_3 are initially in a trigonal coordination, as shown by IR and UV-Vis spectroscopy, respectively. The coordination of a weak ligand like the CO molecule indicates that such trigonal species are probably rather distorted and reactive.

Acknowledgements

Authors thank Dr. Mauro Raimondo (Politecnico di Torino, Italy) for FESEM measurements.

References

1. A. Frache, E. Gianotti and L. Marchese, *Catal. Today*, 2003, **77**, 371.

2. L. Marchese, J. Chen, J. M. Thomas, S. Coluccia, A. Zecchina, *J. Phys. Chem*., 1994, **98**, 13350.

3. M. Vishnuvarthan, V. Murugesan, E. Gianotti, L. Bertinetti, S. Coluccia and G. Berlier, *Microporous Mesoporous Mater*., 2009, **123**, 91.

4. J. Chen and J. M. Thomas, *J. Chem. Soc., Chem. Commun*.,1994, 603.

5. S. Hocevar, J. Batista and V. Kucic, *J. Catal*., 1993, **139**, 351.

6. W. Fan, B. M. Weckhuysen, *Journal of Nanoscience and Nanotechnology*, 2003, **3**, 271.

7. B. Bonelli, M. Armandi, S. Hernandez, S. Vankova, E. Celasco, M. Tomatis, G. Saracco and E. Garrone, *Phys. Chem. Chem. Phys*., 2014, **16**, 7074.

8. S. Zanarini, S. Vankova, S. Hernandez, V.S. Ijeri, M. Armandi, E. Garrone, B. Bonelli, B. Onida, P. Spinelli, *Chem. Commun*., 2012, **48**, 5754.

9. M. Armandi, S. Hernandez, S. Vankova, S. Zanarini, B. Bonelli, E. Garrone, *ACS Catalysis*, 2013, **3**, 1272.

10. S. Hernández, S. Bensaid, M. Armandi, A. Sacco, A. Chiodoni, B. Bonelli, E. Garrone, C.F. Pirri, G. Saracco, *Chem. Eng. J.*, 2014, **238**, 17.

11. R. Zha, M. Dong, Z. Qin, J. Wang a, *Mater. Lett*., 2008, **62**, 4573.

12. A. Manjón-Sanz, M. Sánchez- Sánchez E. Sastre, *Catal. Today*, 2012, **179**, 102.

13. L. Zhou, T. Lu, J. Xu, M. Chen, C. Zhang, C. Chen, *Microporous Mesoporous Mater*., 2012, **161**, 76.

14. K. Iwakai, T. Tago, H. Konno, Y. Nakasaka, T. Masuda, *Microporous Mesoporous Mater*., 2011, **141**, 167.

15. T. Tago, M. Nishi, Y. Kono, T. Masuda, *Chem. Lett*., 2004, 1040.

16. T. Tago, K. Iwakai, M. Nishi, T. Masuda, *J. Nanosci. Nanotechnol*., 2009, **9**, 612.

17. C. Montes, M.E. Davis, B. Murray, M. Narayana, *J. Phys. Chem*., 1990, **94**, 6425

18. V. Kurshev, L. Kevan, D.J. Parillo, C. Pereira, G.T. Kokotailo, R.J. Gorte, *J. Phys. Chem*., 1994, **98**, 10160.

19. S. Esposito, M. Turco, G. Ramis, G. Bagnasco, P. Pernice, C. Pagliuca, M. Bevilacqua, A. Aronne, *Journal Solid State Chem.*, 2007, **180**, 3341.

20. A. Verberckmoes, M. Uytterhoeven, R. Schoonheydt, *Zeolites*, 1997, **19**, 180.

21. G. Lehman, *J. Phys. Chem. Solids*, 1969, **30**, 395.

22. S. Thomson, V. Luca and R. Howe, *Phys. Chem. Chem. Phys*.,1999, **1**, 615.

23. J. Šponer, J. Čejka, J. Dědeček, B. Wichterlová, *Microporous Mesoporous Mater*., 2000, **37**, 117.

24. P.A., Barrett, G. Sankar, C. Richard, A. Catlow, J.M. Thomas, *J. Phys. Chem*., 1996, **100**, 8977.

25. K. Chakarova, K. Hadjiivanov, *Microporous Mesoporous Mater*., 2009, **123**, 123.

26. F. Geobaldo, B. Onida, P. Rivolo, F. Di Renzo, F. Fajula, E. Garrone, *Catal. Today*, 2001, **70**, 107.

27. H. F. W. van Breukelen, G. J. C. Kraaijveld, L. J. M. van de Ven, J. W. de Haan, J. H. C.van Hooff, *Microporous Mater.*, 1997, **12**, 313.

28. K. I. Hadjiivanov, G. N. Vayssilov, *Adv. Catal.*, 2002, **47**, 307.

29. M. Zayat, D. Levy, *Chem. Mater.*, 2000, **12**, 2763.

30. N. N. Greenwood, A. Earnshaw, *Chemistry of Elements*, Elsevier 1997.

Caption to Figures and Schemes

Scheme 1 Reversible redox process concerning tetrahedral Co ions within the Co-APO-5 framework.

Scheme 2 Cobalt species formed by thermal oxidative treatment of CoAPO-5 powder.

Scheme 3 Coordination of a ligand M on the trigonal specie D.

Figure 1. XRD patterns of calcined CoAPO-5-N powder.

Figure 2. FE-SEM micrographs of CoAPO-5-C (a) and CoAPO-5-N (b)

Figure 3. DR-UV-Vis spectra of CoAPO-5-N powder (section a) and CoAPO-5-C (section b): dried sample (solid black line); calcined sample (dashed line); sample dehydrated at 423 K (solid grey line).

Figure 4. IR spectra in the 975-800 cm^{-1} range concerning CoAPO-5-N (curves 1 and 2) and CoAPO-5-C (curves 3 and 4) outgassed at 423 K (dotted curves) and 523 K (continuous curves).

Figure 5. Difference IR spectra in the 2225-2050 cm^{-1} range obtained after dosing CO on sample CoAPO-5-N outgassed at 523 K. Inset: same IR spectra in the 950-800 cm^{-1} range. CO equilibrium pressures in the 0.10-15 mbar range. Difference IR spectra were obtained after subtraction of spectra of the bare samples outgassed at 523 K.

Figure 6. Difference IR spectra in the 2225-2050 cm^{-1} range obtained after dosing CO on sample CoAPO-5-C outgassed at 523 K. Inset: same IR spectra in the 950-800 cm^{-1} range. CO equilibrium pressures in the 0.10-15 mbar range. Difference IR spectra were obtained after subtraction of spectra of the bare samples outgassed at 523 K.

Figure 7. DR-UV-Vis spectra of CoAPO-5-N (a) and CoAPO-5-C (b) powders obtained on calcined sample (dashed line), on sample outgassed at 423 K (continuous grey line) and after dosing 30 mbar NH_3 on the sample dehydrated at 423 K (continuous black line).

Figure 8. Cumulative amounts of evolved O_2 for: CoAPO-5-N (circles), CoAPO-5-C (triangles), control experiment without catalyst (crosses).

Table 1. Textural features of the samples as determined by adsorption/desorption isotherms of N_2 at 77 K.

Sample	**BET SSA (m^2/g)**	**Langmuir SSA (m^2/g)**	**Total pore volume (cm^3/g)**	**Micropores Volume (cm^3/g) [a]**	**External Surface Area (m^2/g)[a]**
CoAPO-5-C 3 wt%	283	340	0.12	0.12	3.7
CoAPO-5-C 1.9 wt%	216	270	0.125	0.091	13
CoAPO-5-C 0.96 wt%	170	220	0.087	0.067	21
CoAPO-5-N 1.9 wt%	242	291	0.121	0.092	34

[a] As obtained according to the t-plot method.

Table 2. Elemental analysis using SEM-EDX on 10-50 nm diameter spots.

Sample	Co (wt%)			
	Spot 1	Spot 2	Spot 3	Spot 4
CoAPO-5-C 1.9 wt%	3.70	0.53	2.87	0.73
CoAPO-5-N 1.9 wt%	2.08	1.82	2.02	1.57

Scheme 1

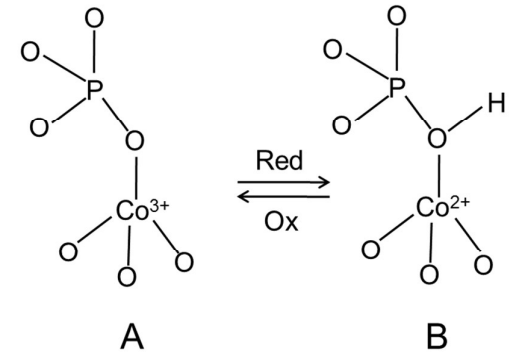

Scheme 2

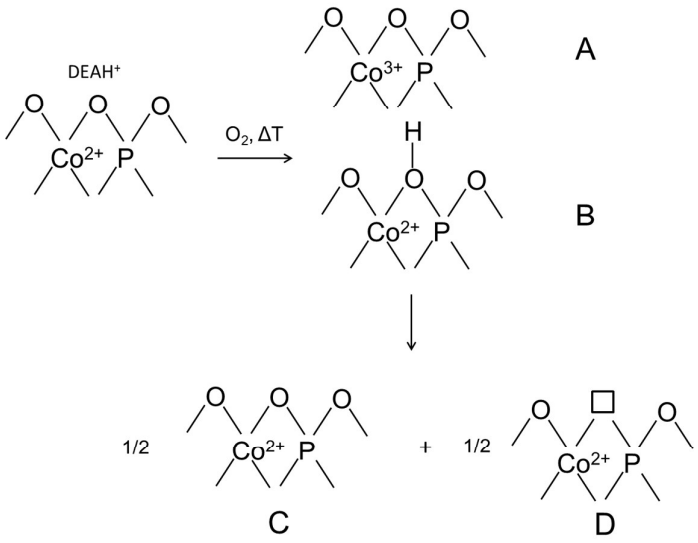

Scheme 3

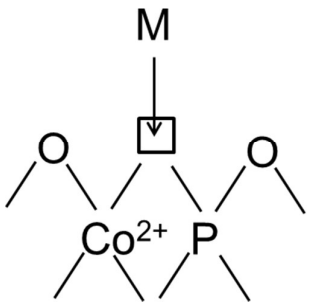

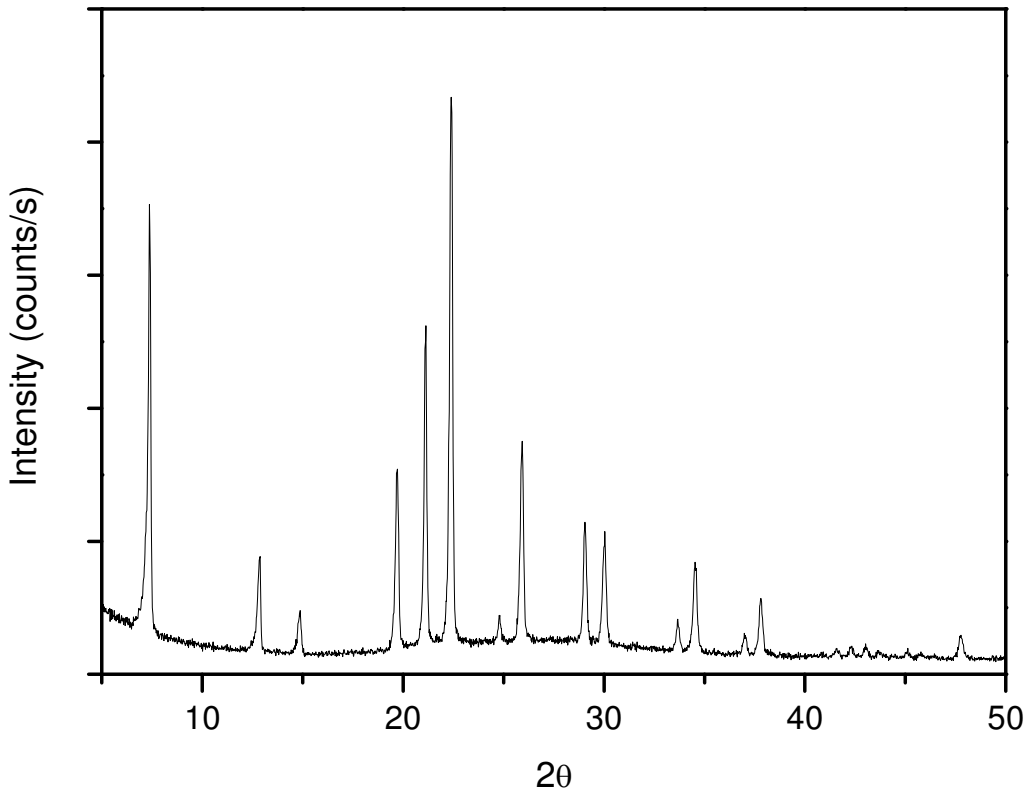

Figure 1

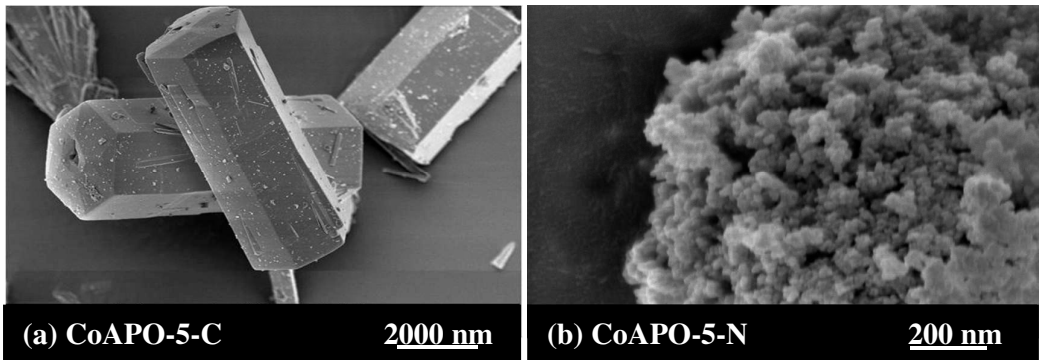

Figure 2

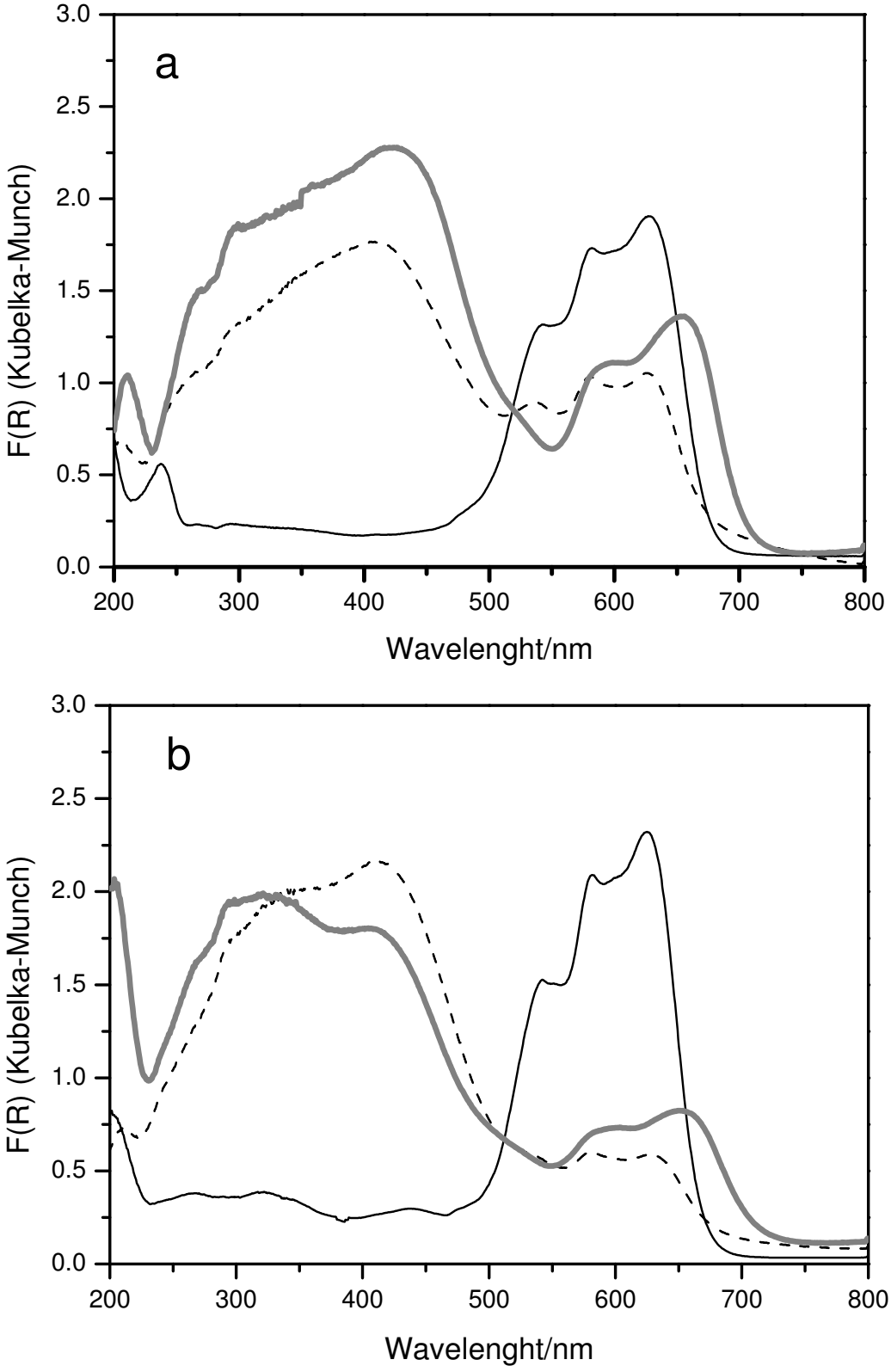

Figure 3

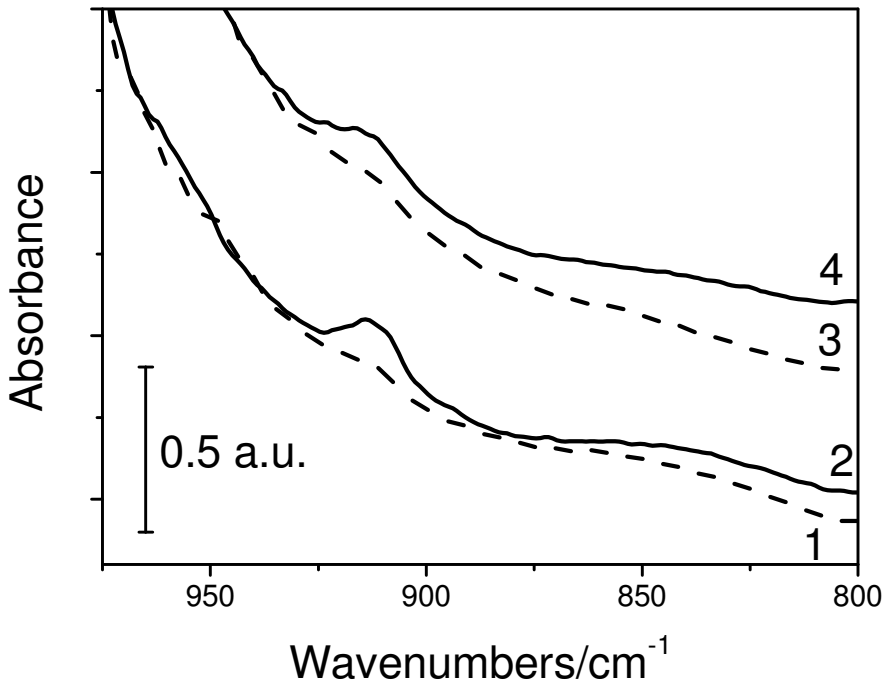

Figure 4

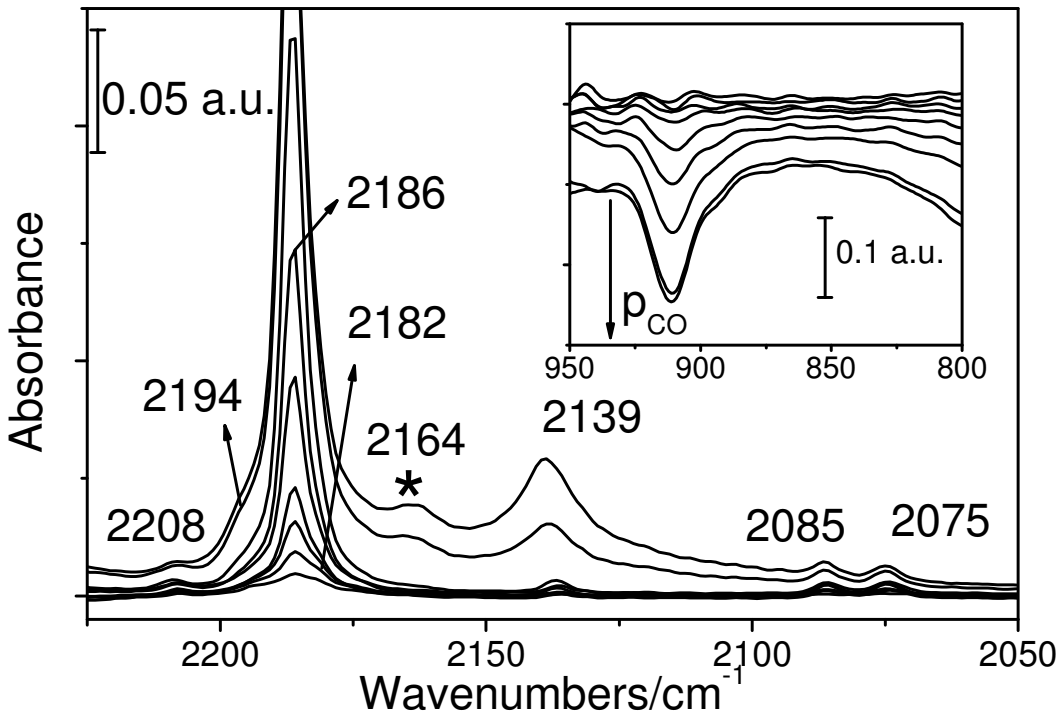

Figure 5

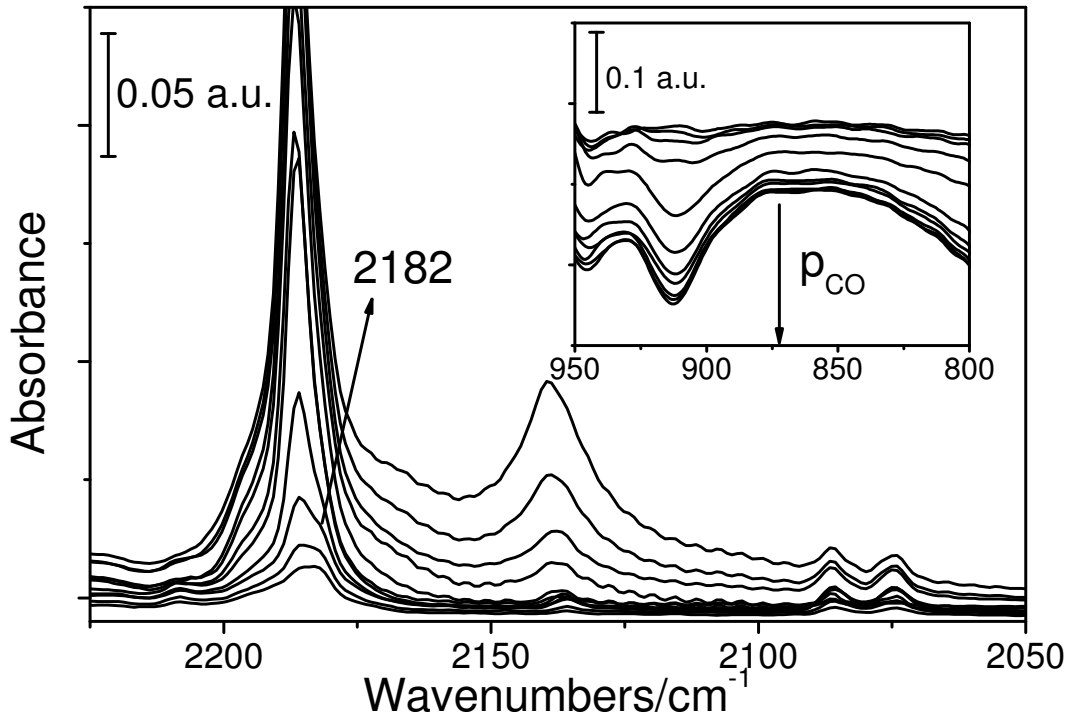

Figure 6

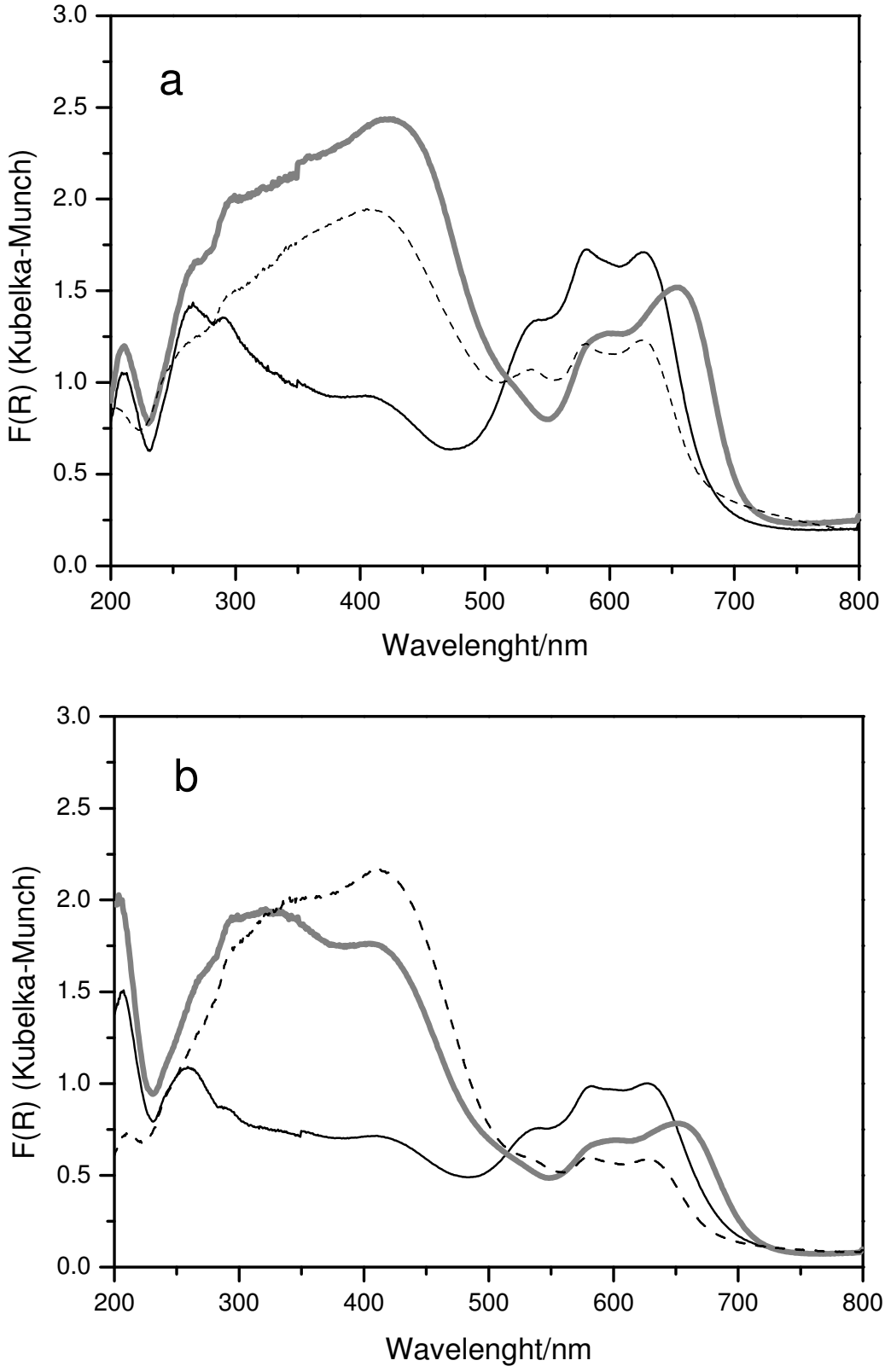

Figure 7

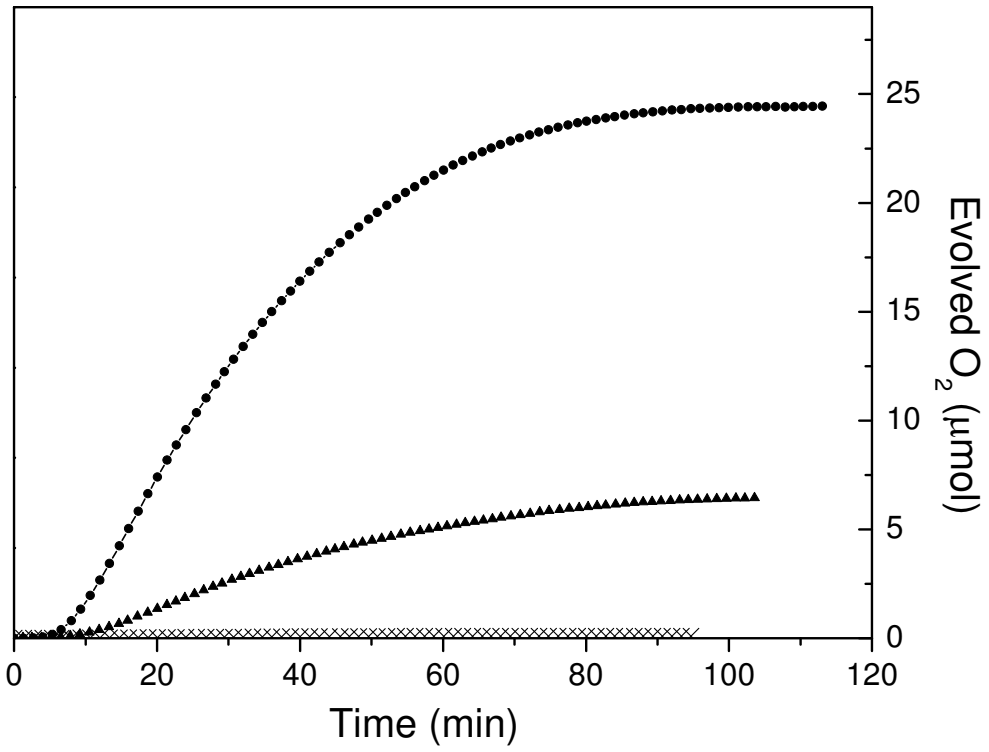

Figure 8

Graphical Abstract

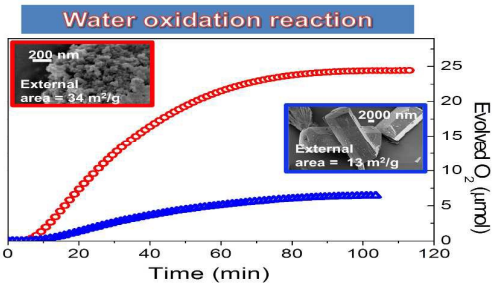

The synthesis of nanosized CoAPO-5 particles brings to a fourfold increase in the rate of the water oxidation reaction with respect to the sample prepared by conventional synthesis.